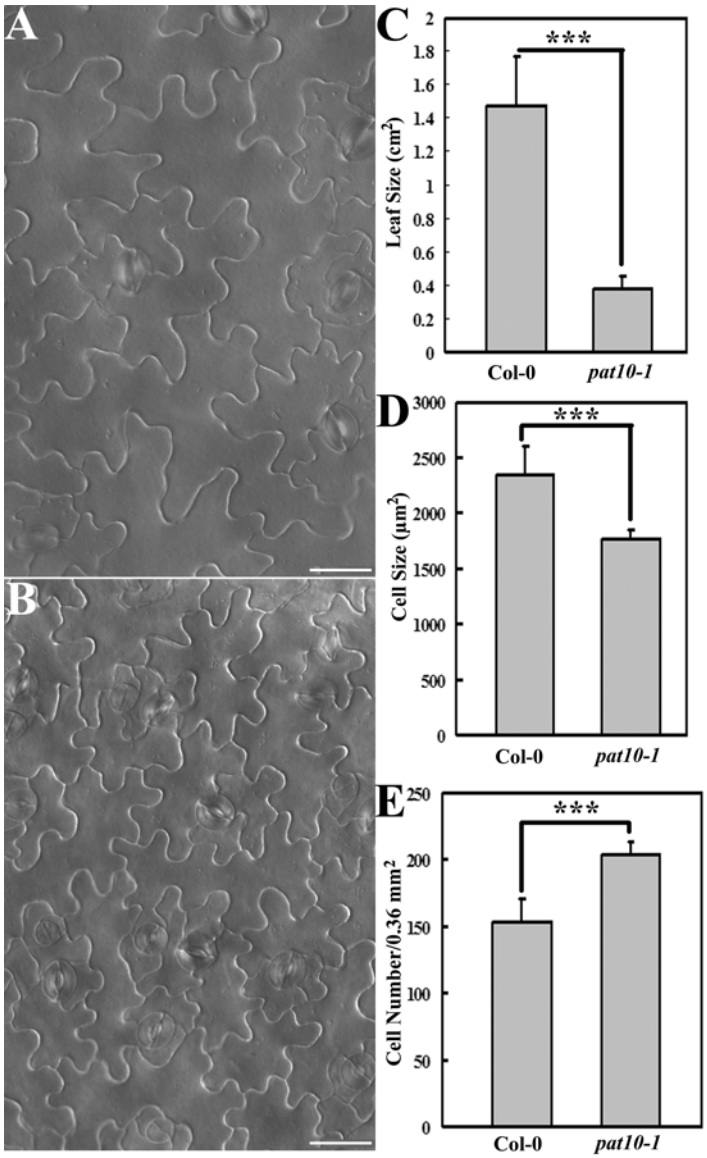

Supplemental Figure 1. Cell size and number were both reduced in *pat10*.

(A) and (B) Representative images of epidermal cells from the 4th pair of true leaves of wild type (A) or of *pat10* mutants (B) at 20 DAG. Bars = 10 μm.

(C) Leaf size (cm^2).

(D) Cell size (μm^2).

(E) Quantification of average cell number/0.36 mm^2. 20 images from 10 leaves were analyzed using ImageJ.

Results shown in (C), (D) and (E) are given as means ± standard error (SE). Asterisks indicate significant difference (Student's *t*-test, P<0.01). Bars = 20 μm.

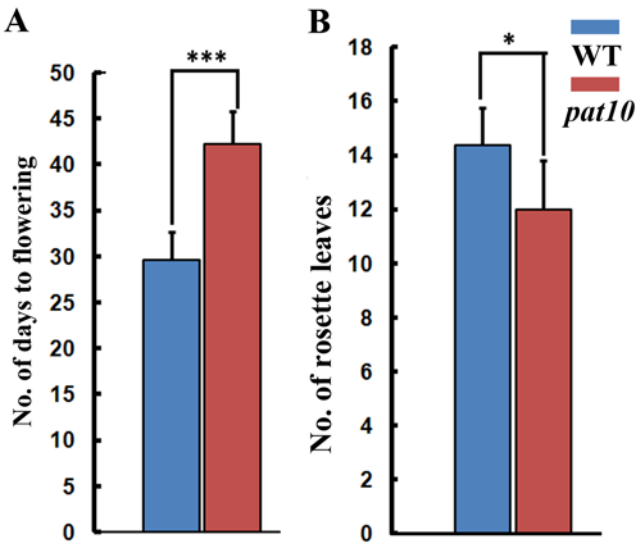

Supplemental Figure 2. *PAT10* mutations caused temporally delayed but developmentally early floral transition.

(A) and (B) Number of days to flowering (A) and number of rosette leaves at floral transition (B) in wild type and in *pat10* mutants. Data were collected from 30 long-day-grown plants for each genetic background. Results are given as means ± standard deviation (SD). Asterisks indicate statistical significance: one indicates $P<0.05$ while three indicate $P<0.01$ (Student's *t*-test).

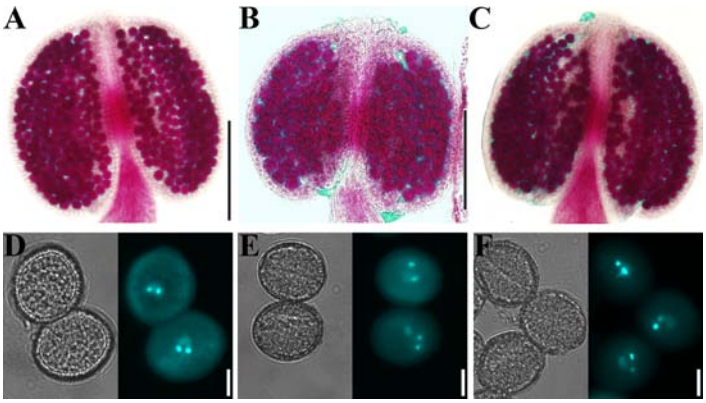

Supplemental Figure 3. Pollen viability was not affected by *PAT10* mutations.

(A) to (C) Alexander staining of mature anthers from wild type (A), heterozygous *pat10* mutants (B) and homozygous *pat10* mutants (C). Bars = 200 μm.

(D) to (F) Nuclear staining of mature pollen from wild type (D), heterozygous *pat10* mutants (E) and homozygous *pat10* mutants (F). Bright field images and DAPI staining images are placed side by side. Bars of insets = 10 μm.

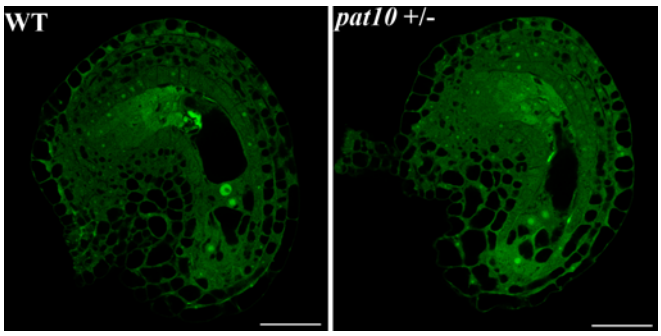

Supplemental Figure 4. Embryo sac was normal in ovules from heterozygous *pat10* mutants. Representative ovule from mature pistils of wild type (WT) or heterozygous pat10 mutants (*pat10* +/-) are shown (n=20). Bars = 25 μm.

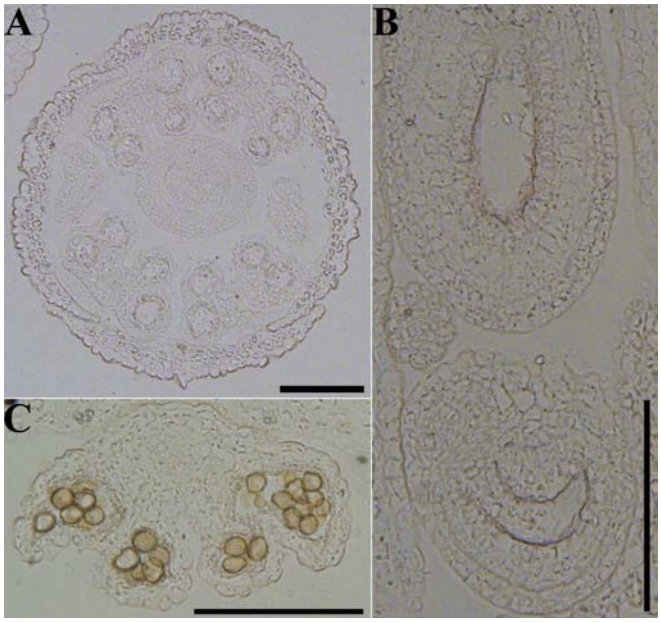

Supplemental Figure 5. The probe used in RNA *in situ* hybridization was specific for *PAT10*.

(A) A stage 5-6 *pat10-1* anther labeled by the antisense probe (A).

(B) Longitudinal section of a pistil from *pat10-1* plants labeled by the antisense probe.

(C) A stage 9 *pat10-1* anther labeled by the antisense probe

Bars = 100 μm.

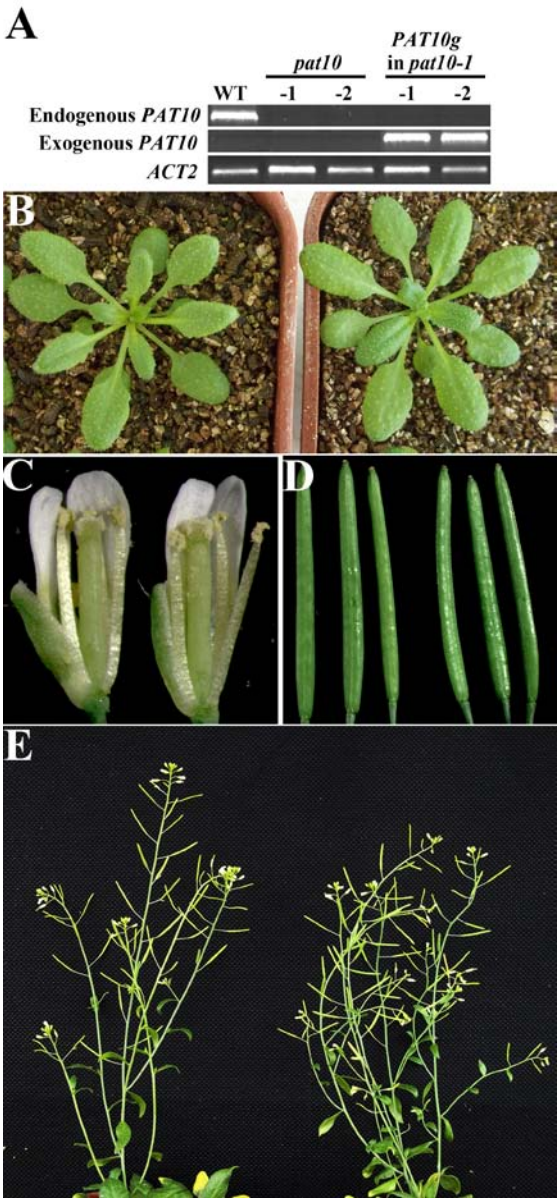

Supplemental Figure 6. *PAT10*-GFP complemented *pat10*.

(A) Transcript analysis showing that the complemented lines (two independent transgenic lines expressing *PAT10*-GFP in *pat10-1*) expresses exogenous *PAT10* but not endogenous *PAT10*. *ACT2* was used as the internal control. (B) Representative vegetative growth of wild type (right) and *PAT10*-GFP; *pat10-1* transgenic plants (left). (C) Representative open flowers of wild type (right) and *PAT10*-GFP;*pat10-1* transgenic plants (left). (D) Representative mature siliques of wild type (right) and *PAT10*-GFP;*pat10-1* transgenic plants (left). (E) Representative reproductive growth of wild type (right) and *PAT10*-GFP;*pat10-1* transgenic plants (left).

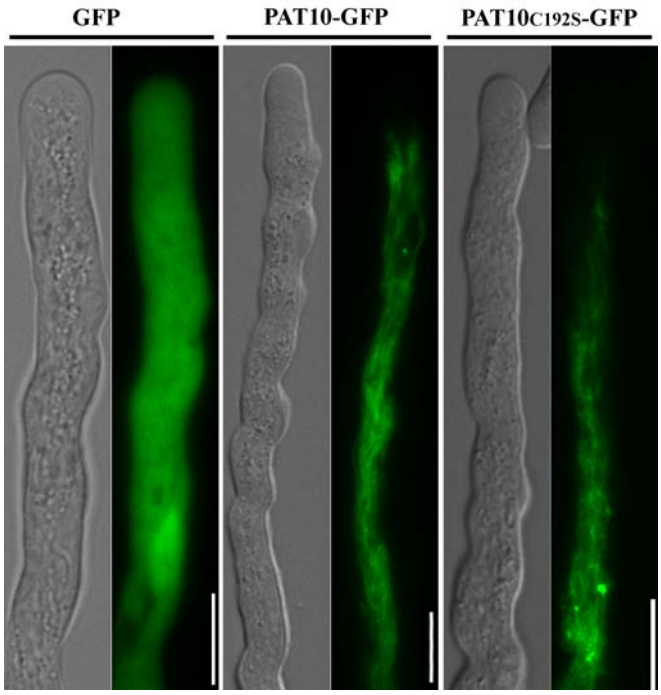

Supplemental Figure 7. Subcellular localization of PAT10 and PAT10$_{C192S}$ in transgenic Arabidopsis pollen tubes growing *in vitro*.

Representative pollen tubes from stable transgenic plants expressing either soluble GFP, PAT10-GFP or PAT10$_{C192S}$-GFP. Bright field images and fluorescent images are placed side by side. Bars = 10 μm.

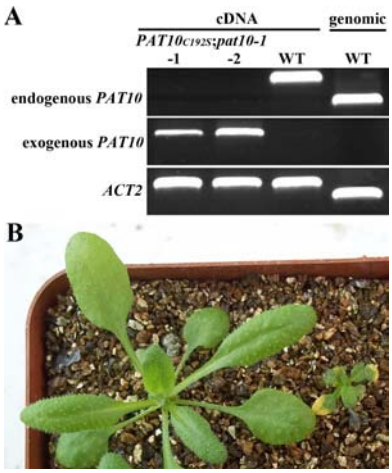

Supplemental Figure 8. *PAT10*$_{C192S}$-GFP did not complement *pat10*.

(A) Transcript analysis showing that the *PAT10*$_{C192S}$-GFP transgenic line expresses exogenous *PAT10*$_{C192S}$ but not endogenous *PAT10*. *ACT2* was used as the internal control.

(B) Representative vegetative growth of wild type (right) and *PAT10*$_{C192S}$-GFP; *pat10-1* transgenic plants (left).

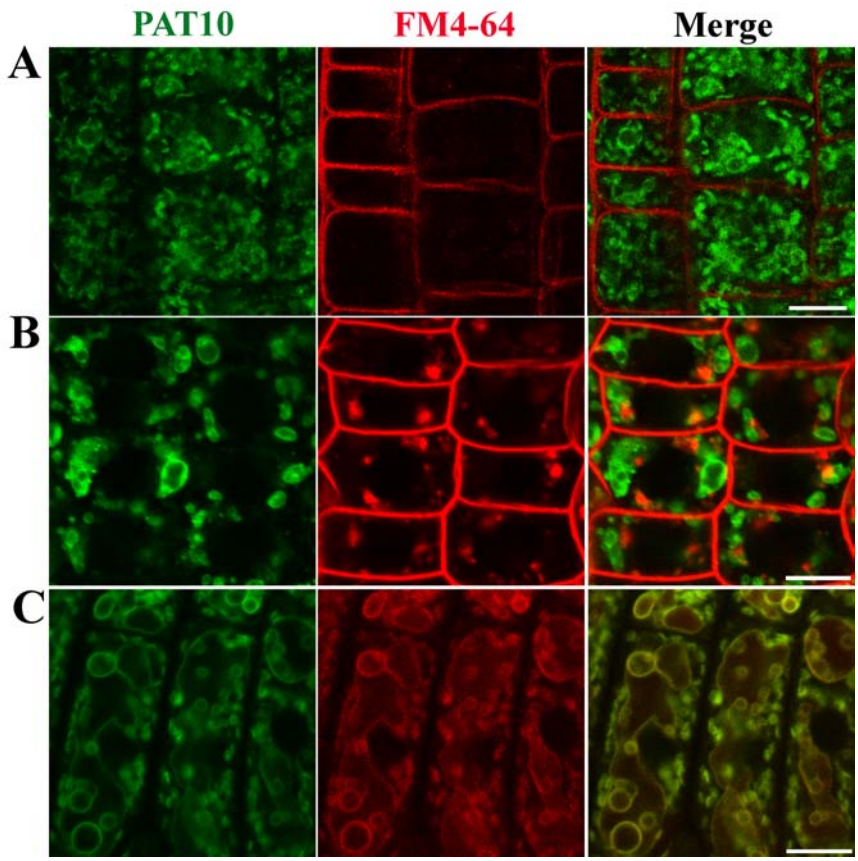

Supplemental Figure 9. PAT10 localizes at the tonoplast.

(A) *PAT10*-GFP (green) transgenic roots immediately after 1 min incubation with MS media supplemented with 4 µm FM4-64 (red).

(B) *PAT10*-GFP (green) transgenic roots treated with FM4-64 (red) and BFA. FM4-64 forms BFA-compartments while PAT10 still presents at tonoplast. Roots were treated first with 4 µM FM4-64 for 5 min, then washed and incubated with MS medium supplemented with 50 µM BFA for 50 min and visualized for the formation of BFA compartments.

(C) *PAT10*-GFP (green) transgenic roots 3 hr after FM4-64 (red) treatment when FM4-64 is fully incorporated at tonoplast. Bars = 7.5 µm.

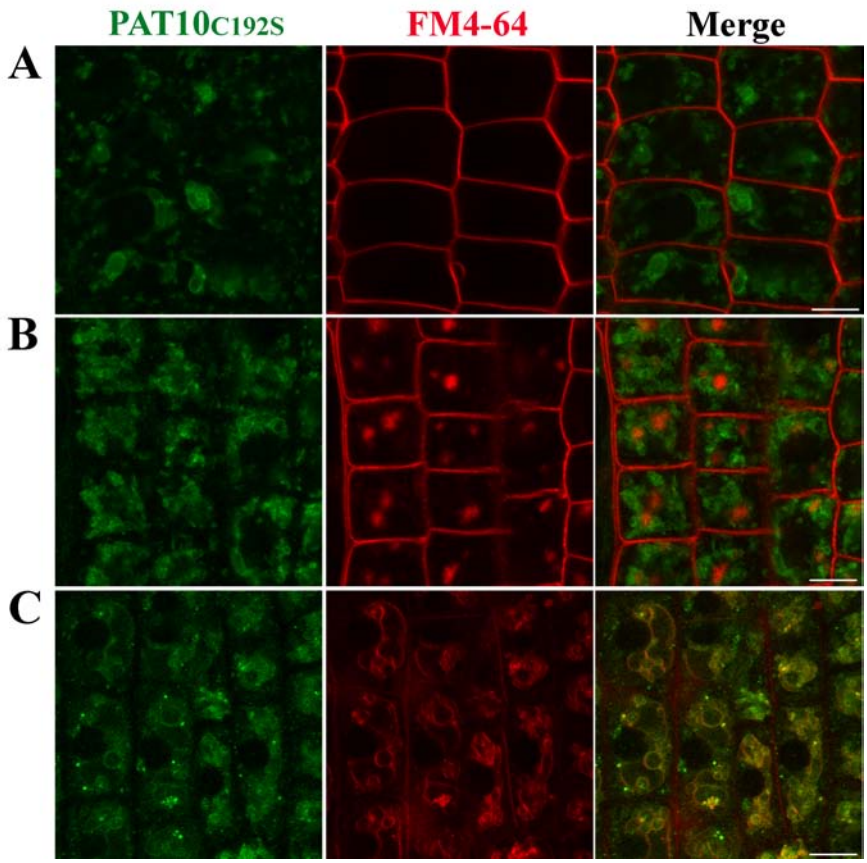

Supplemental Figure 10. $PAT10_{C192S}$ localizes at the tonoplast as well as BFA-sensitive vesicles.

(A) *PAT10*$_{C192S}$-GFP (green) transgenic roots immediately after 1 min incubation with MS media supplemented with 4 µm FM4-64 (red).

(B) *PAT10*$_{C192S}$-GFP (green) transgenic roots treated with FM4-64 (red) and BFA. FM4-64 forms BFA-compartments. A substantial fraction of *PAT10*$_{C192S}$-GFP is present not only at tonoplast but also at the aggregates surrounding FM4-64-aggregates. Roots were treated first with 4 µM FM4-64 for 5 min, then washed and incubated with MS medium supplemented with 50 µM BFA for 50 min and visualized for the formation of BFA compartments.

(C) *PAT10*$_{C192S}$-GFP (green) transgenic roots 3 hr after FM4-64 (red) treatment when FM4-64 is fully incorporated at tonoplast. Beside its tonoplast localization, *PAT10*$_{C192S}$--GFP is present in punctate vesicles not labeled by FM4-64. Bars = 7.5 µm.

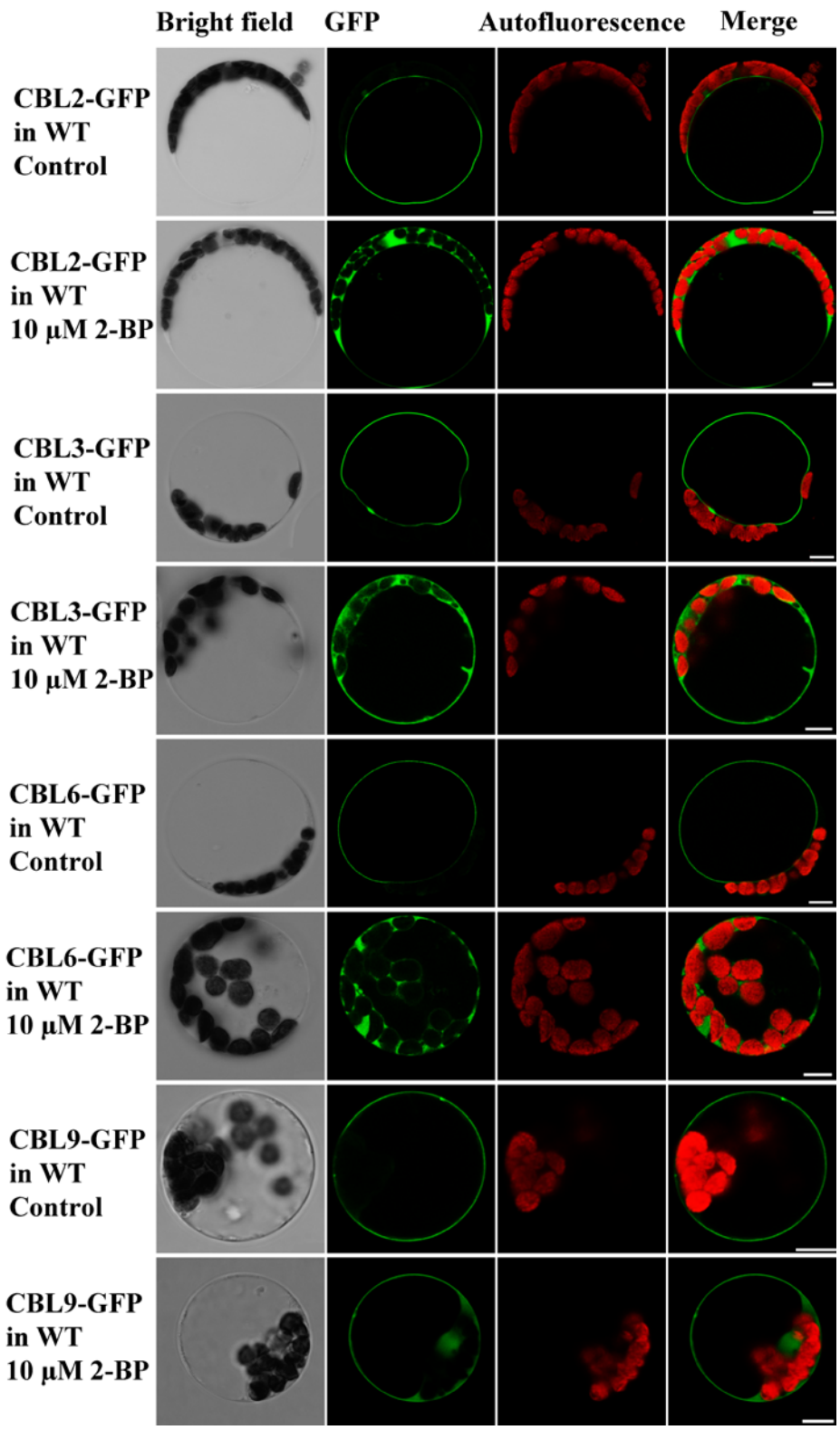

Supplemental Figure 11. Treatment with 2-bromopalmitate (2-BP) abolished the membrane association of CBL2, CBL3, CBL6 and CBL9 in wild-type protoplasts. Representative images from three independent experiments are shown. In total, 60-80 protoplasts were visualized for each expression. 2-BP is for 2-bromopalmitate. Bars= 7.5 µm.

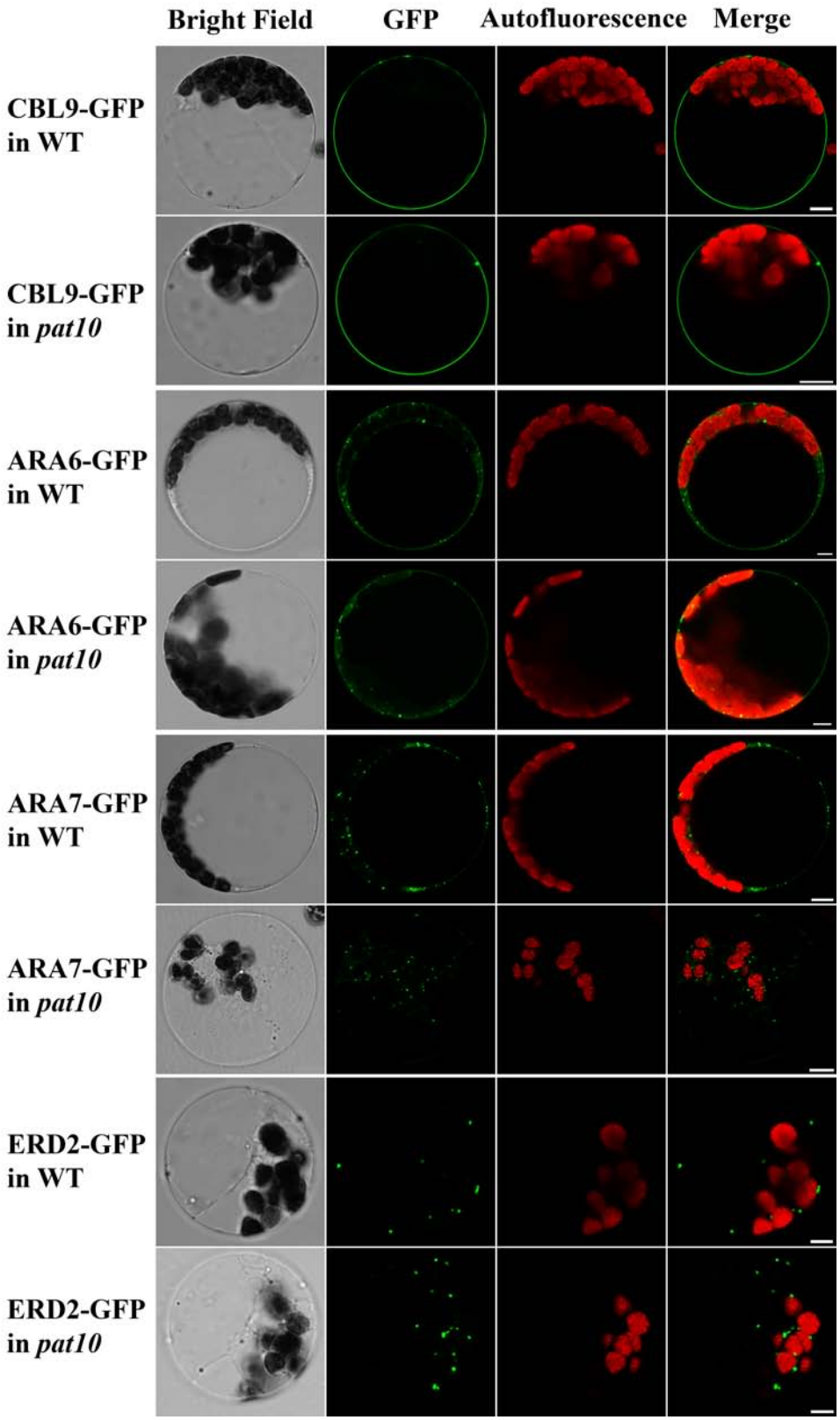

Supplemental Figure 12. Membrane association of CBL9, ARA6, ARA7 and ERD2 did not rely on functional *PAT10*. Representative images from three independent experiments are shown. In total, 60-80 protoplasts were visualized for each expression. Bars= 5 μm for ARA6 and ERD2. Bars= 7.5 μm for ARA7 and CBL9.

Supplemental Table 1. Primers used in this study.

Oligos	5'-3' sequences
G1	ATTTGACATGCGGCTATTGTC
G2	GAAGATCTGGAGGAGTCGCTC
G3	ATTTTGCCGATTTCGGAAC
G4	GAAGATCTGGAGGAGTCGCTC
G5	AACGTCCGCAATGTGTTATTAAGTTGTC
R1	ATTTGACATGCGGCTATTGTC
R2	GAATTTACTATGGTTTTTCTGGCC
R3	CATATCGATGCAGGTGTAGGG
R4	TTCTGGTGGTACATCTGTGAAGAG
R5	TTCTGGTGGTACATCTGTGAAGAG
R6	GAAGATCTGGAGGAGTCGCTC
R7	TGAACTTGTGGCCGTTTACGT
RD29A-F	GTTACTGATCCCACCAAAGAAGA
RD29A-R	GGAGACTCATCAGTCACTTCCA
RD20-F	TTAGCTCCGGTCACCAGTCA
RD20-R	CATGTATGGTTTTGGTAATGTTTCC
ERD10-F	TCTCTGAACCAGAGTCGTTT
ERD10-R	CTTCTTCTCACCGTCTTCAC
RAB18-F	GGCTTGGGAGGAATGCTT
RAB18-R	TTGATCTTTTGTGTTATTCCCTTCT
GAPDH-F	TGAAATCAAAAAGCTATCAAGG
GAPDH-R	CATCATCCTCGGTGTATCCAA
TUBLIN2-F	ATCCGTGAAGAGTACCCAGAT
TUBLIN2-R	AAGAACCATGCACTCATCAGC
PAT10gF	CACCGTTTATGGGTGGATCTTGTCTTC
PAT10gR	CGCAGCAGCGACATTTCAAC
PAT10gmF	GAACATGTATAGGCCAGAAAAACC

PAT10gmR	CTAACCAAACACTGTGATGATCAAACTGAAG
ProF	CACCGAGGACGTCTAAGGAAACGTAAA
ProR	GTTTTGGTTTGACTCTCTCTCTTTC
ProbeF	CTGGTGGTACATCTGTGAAG
ProbeR	CGTCTCACAAGTTCATAAGTGC
CBL2-F	CACCATGTCGCAGTGCGTTGAC
CBL2-R	GGTATCTTCAACCTGAGAATGG
CBL3-F	CACCATGTCGCAGTGCATAGACGG
CBL3-R	GGTATCTTCCACCTGCGAGTG
CBL6-F	CACCATGATGATGCAATGTTTAGATGG
CBL6-R	TCCATCCAGCTCACTAGGAG
CBL9-F	CACCATGGGTTGTTTCCATTCCACG
CBL9-R	CGTCGCAATCTCGTCCACC
ERD2-F	CACCATGATATCTTTAGATTTGC
ERD2-R	AGCCGGAAGCTTAAGTTTGGTG